E-ISSN: 2706-8927
P-ISSN: 2706-8919
www.allstudyjournal.com
IJAAS 2021; 3(2): 161-167
Received: 10-02-2021
Accepted: 12-03-2021

Sorgul Kashmiri
Senior Teaching Assistant Professor, Lecturer at Physic Department, Balkh University, Afghanistan

Abdulwahed Qaderi
Junior Assistant professor Lecturer at physic department Balkh University, Afghanistan

Mir Mohammad Zaher Haidari
Professor, Lecturer at Physic Department, Balkh University, Afghanistan

Corresponding Author:
Sorgul Kashmiri
Senior Teaching Assistant Professor, Lecturer at Physic Department, Balkh University, Afghanistan

Heat capacity analysis of armchair nano-ribbons in magnetic fields

Sorgul Kashmiri, Abdulwahed Qaderi and Mir Mohammad Zaher Haidari

Abstract
Background: Thermodynamic properties of graphene-based armchair nano-ribbons and their magnetic susceptibility were studied in this research.
Methodology: This research is applied in terms of its type and cognitive in terms of approach. To this end, a Hamiltonian tight-binding model was used to describe the dynamic of electrons in the device. Energy bands of the sample obtained by Hamiltonian diagonalization. The density of energy states has obtained by using these energy bands.
Findings: Magnetic susceptibility and heat capacity were obtained by using energy integration on states' density function and Dirac function. The numerical results of heat capacity and magnetic susceptibility were obtained in different temperatures, gaps, chemical potentials, and widths.
Conclusion: It is concluded that the heat capacity and state density of armchair nano-ribbon is influenced by the width of ribbons, chemical potential, and energy gap. Any change in the energy gap, chemical potential, and the width of the ribbon will lead to a significant change in the density of states and the heat capacity of the armchair nano-ribbon.

Keywords: armchair, nano-ribbons, magnetic susceptibility

Introductions

The nanomaterial is the material that at least one of its dimensions is in a 1 to 100nm scale. This topic relates to nanotechnology issues. Nanotechnology is the technology for the production and manufacture of new materials, tools, and systems in nanometer-scale i.e. atomic and molecular levels. They are important in modern technology by having control over the nanometer scale and using these properties [1]. A nanometer is 10^{-9}m. This is 18000 times smaller than the diameter of a human hair. Generally, nanotechnology is about expanding, producing, and using tools and materials with 1 to 100nm dimensions. Nanotechnology divides into three categories: materials, tools, and systems. Materials that are used in nanoscale in nanotechnology are nanomaterial [2]. Nanostructure material is any material that at least one of its dimensions is in the nanometer scale (lower than 100nm). This definition contains all types of structures, including human-made or natural.

Most nanomaterials are zero dimension materials that include NMs with all dimensions in 1-100nm range. NMs have a needle or rod-like dimension, for example with 100nm to 10µm length and include nanotubes, nanorods, and nanowires. Two-dimensional NMs show the sheet-like forms including nano-cover, nano-filters, and nano-layers. Zero-dimensional, one-dimensional, and two-dimensional NMs can be used on the substrate or they can be distributed in the liquid or solid matrix [1]. Three-dimensional NMs can have three optional dimensions with a nano-crystal multilayer structure [1]. These NMs may include bulk powders, nano packages, nano multilayer, nanoparticle dispersion, and nanotubes [3]. Metal-based NMs include quantum dots, nanotube, nanosilver, and nanometer oxides (for example, titanium dioxide, zinc oxide, and ferric oxide). Quantum dots are 2-10nm fluorescent semiconductors. Quantum dots are characterized by a wide absorption spectrum and narrow emission spectrum related to their size. The properties of composite NMs can be designed according to their application to need; these properties depend on the selection of matrix, sintering, form and direction [3]. Modern scientists can produce various materials in nano-scale including light-weight and robust nanoclays, nanofibers, graphene, and carbon nanotubes that can expand more on the light spectrum and significant chemical reaction [4]. Scientists have found some links between exposure of infants (first month after birth) to NMs and exacerbation of asthma, reduction of lung capacity, wheezing and coughing

Without infection. However, nanotechnology may provide an excellent opportunity to treat pediatric diseases with great promise in imaging and medical applications [5]. Inhaled NMs can be delivered in the body through circulation. Epidemiologic studies have reported that severe cardiovascular complications like changing the blood coagulation may change the frequency and function of the heart. This may happen due to exposure to NMs. Besides, chronic exposure to NMs can reduce Forced Expiratory Volume (FEV) and Forced Vital Capacity (FVC). In an animal model study, Beker *et al.* (2011) concluded that carbon nanotubes and TiO_2 nanoparticles may develop a tumor. Engineered nanotubes have poisonous effects on fibroblasts and epidermal keratinocytes. They can also change the gene or protein state [6]. Despite such advancement in NMs technology, there is not yet enough information about the effect of NMs on human health. NMs may not detect after discharging into the environment and they may cause various problems, including environmental problems [7]. Therefore, further studies are required to systematically explain the basic functional structure of NMs by considering their chemistry. Besides, risk assessments should be done on NMs. One risk is being exposed to these materials during production or use. Therefore, nano-science has been recommended to reduce the environmental and human health risks caused by the production and use of NMs and progress the new environment-friendly products. Major concerns about nanotechnology applications include unknown environmental effects, waves in the environment, sedimentation, detection limitations, and high costs of renewal and depositing in the environment [8].

Nanostructures

Nano-ribbons are structures that narrowed down along the sheet and there are unsaturated carbon atoms at their edges as hanging. These narrow elongated carbon nano-ribbons were discovered by Andre Geim and Konstantin Novoselov in 2004 [9]. Nano-ribbons' edges create electronic, chemical, and magnetic properties that are very different from the bulk state based on the type and size of the edges. Electronic states of graphene nanoribbons were studied by Fujita et.al and introduced as a theoretical model [10]. Regarding the direction of carbon atoms on the edge of graphene sheets and considering that cut direction of the graphene sheet, zigzag (ZGNR) and armchair (AGNR) graphene nano-ribbons develop. Electronically, graphene is a metalloid with a zero energy gap. On the contrary, graphene nano-ribbons can show metallic or semi-conduction properties based on their edge. Zigzag nanoribbons are always metallic while armchair nanoribbons can be metallic or semi-metallic depending on their edge. Zigzag and armchair nanoribbons are shown in the following figure.

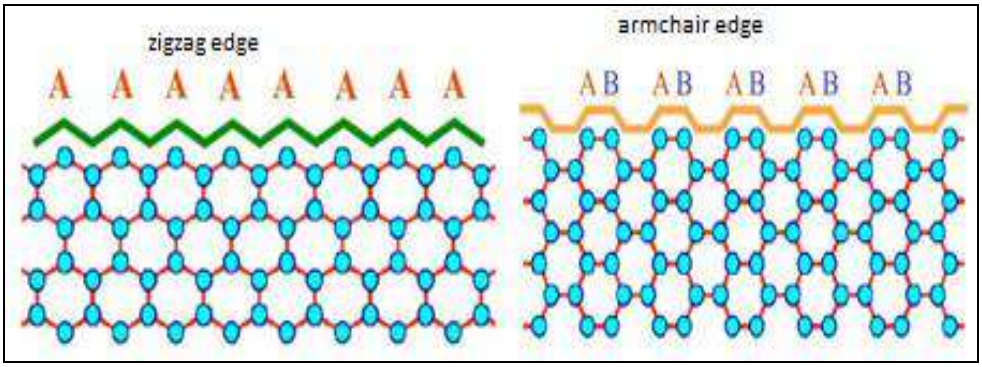

Fig 1: Graphene nanoribbons

Zigzag edge shows the local state while armchair edges have not such state. Graphene edge states are the origin of magnetic and transportation properties in the nano scale. Graphene nanoribbon model is suitable to analyze electron states. We can define crystal momentum (k wavenumber) due to the frequency along with the length of the nanoribbon. The vectors for armchair and zigzag nanoribbons are $\left(a=\sqrt{3},a,0\right)$ and $a=(a,0)$, respectively. The width of nanoribbon can be defined with n. Note that the same n number for both armchair and zigzag nanoribbons does not produce nanoribbons with equal widths when they are measured with the same units. Therefore, when we want to consider the physical values of zigzag and armchair nanoribbons with same W width, we use the following equation [11]:

$$W=\begin{cases}(N+1)\frac{1}{2}a\equiv Wa\rightarrow Armchair\\ \frac{\sqrt{3}}{2}Na+\frac{a}{\sqrt{3}}\equiv Wz\rightarrow Zigzag\end{cases} \quad (1)$$

Materials and Methods

This research is applied in terms of its type and cognitive in terms of approach. A tight-binding Hamiltonian model was used to describe the electron dynamics of the system. Then, the energy bands of this sample obtained by Hamiltonian diagonalization. The system energy states obtained by using these energy bands.

Problem Formulation

The density of electrons in a specific position in the space is n(r). This can be written based on single-electron wave functions [12].

$$n(r)=2\sum_{i}\psi_i^*(r)\psi_i(r) \quad (2)$$

To facilitate the lengthy calculations caused by the increasing number of electron particles (electrons and ions) and the complexity of quantum devices in the solid mass, we are interested to use second quantization and tight-binding approximation in solving the equations to obtain a Hamiltonian system. Tight-binding Hamiltonian

approximation includes only two expressions (kinetic energy of electrons and electron-ion electrostatic potential). A Hilbert space is required to solve the Schrodinger equation and the energy spectrum of electrons. Therefore, it is necessary to describe the atomic orbital wave functions (Wannier functions). Wannier wave function states that the electron is constrained only to one ion in wave functions obtained by solving the Schrodinger equation [13].

$$|\varphi_i\rangle = |\varphi(r - R_i)\rangle \tag{3}$$

Due to the complete Hilbert space, including atomic orbital wave function, we can find wave functions and Schrodinger equation functions. Hybridization is combining atomic orbital wave functions to receive wave function of that electron for some ions. This combined wave function is wave function hybridization. This sandwiches the Hamiltonian hybrid wave functions between atomic orbitals functions $\langle \varphi_i | H | \varphi_j \rangle$ such that it gives electron jump from one ion to another i.e. it gives electron jump range from ith ion to jth ion [14].

Crystal Hamiltonian

Hamiltonian of an independent single-electron crystal by considering spin energy and ion-electron potential is as follows:

$$H = \frac{p^2}{2m} + \sum_{i,\tau} V(r - R_{i\tau}) \tag{4}$$

Writing Hamiltonian by using the Schrodinger equation for equation (4) gives a non-diagonal matrix that can be diagonalized by changing the bases and going to indirect space. Now, at the first step, we write the proposed wave function to solve $H\psi = E\psi$ equation:

$$\psi_\tau(k,r) = \frac{1}{\sqrt{N}} \sum_i e^{ik.R_i} \varphi_\tau(r - R_i) \tag{5}$$

$\varphi_\tau(r - R_i)$ is electron atomic orbital wave function at the presence of the ion in R_i cell and τ which indicates the base conversion i.e. we transferred it from i atomic orbital base in the direct space to τ and k wave vector that k is the wave function in inverse space. Now we prove that Hamiltonian on k is diameter:

$$H_{kk'}^{\tau\tau'} = \langle \psi_\tau(k,r) | H | \psi_{\tau'}(k',r) \rangle = \delta_{kk'} E_n$$
$$\langle \psi_\tau(k,r) | H | \psi_{\tau'}(k',r) \rangle = \int d^3 r \psi_\tau^*(k,r) \left(\frac{p^2}{2m} + \sum V(r - R_{i\tau}) \right) \psi_{\tau'}(k',r) \tag{6}$$

The above integration is on the electron site variable but by using (5), we can rewrite the Hamiltonian matrix element in Block space [15].

$$\langle \psi_\tau(k,r) | H | \psi_{\tau'}(k',r) \rangle = \frac{1}{N} \sum_{i,j} e^{-ik.R_i} e^{ik'.R_j} \langle \varphi_\tau(r - R_i) | H | \varphi_{\tau'}(r - R_j) \rangle \tag{7}$$

If the beginning basic atom and end basic atom in a cell are identical with the beginning and end basic atom in another cell, the variable change is possible. In other words, only the difference of place of beginning and end cells is important not the origin. Therefore, Hamiltonian form in the new base is as follows:

$$H_{kk'}^{\tau\tau'} = \sum_\Delta e^{ik.\Delta} H^{\tau\tau'}(\Delta) \delta_{kk'}$$
$$\frac{1}{N} \sum_i e^{i(k'-k).R_i} = \delta_{kk'} \tag{8}$$

$H^{\tau\tau'}(\Delta) = \langle \varphi_\tau(r - 0) | H | \varphi_{\tau'}(r - \Delta) \rangle$ in equation (7) is the Hamiltonian matrix element between a unit cell in origin and unit cell τ. In other words, it takes one of the unit cells as the origin and transfers other cells with a transmission vector τ. Hilbert space that is built by ribbon wave functions diagonalize crystal Hamiltonian in tight-binding approximation, i.e.:

$$\langle \psi_n(k) | H | \psi_{n'}(k) \rangle = E_n(k) \delta_{nn'} \tag{9}$$

Therefore, ribbon structure wave functions which diagonalize Hamiltonian are written as follows [26]:

$$\psi_n(k) = \sum_{\tau=1}^m C_{n\tau}(k) \psi_\tau(k) = \frac{1}{\sqrt{N}} \sum_{\tau,i} C_{n\tau}(k) e^{ik.R_i} \varphi_\tau(r - R_i) \tag{10}$$

To obtain eigenvalues of a crystal, the following steps should be considered:

1-selecting reference cell,

2-determining the number of atomic bases

3-obtaining Hamiltonian matrix elements between reference cell and cells in Δ i.e. $H^{\tau\tau'}(\Delta)$ (electron jump range between two atoms located at the base of wave in two neighbor cells).

4-formulating $H^{\tau\tau'} = \sum_\Delta e^{ik.\Delta} H^{\tau\tau'}(\Delta)$ equation, such that it is clear that the number of expressions in the equation depends on the number of neighbor cells. The matrix dimensions obtained by this equation depend on the number of atomic bases. The nearest neighbor approximation is used to calculate Hamiltonian eigenvalues and eigenvectors in a crystal. All jump ranges between far atoms are considered zero in the approximation of the nearest neighbor. The nearest neighbor approximation causes that some matrix elements became zero [16].

5-diagonalizing the obtained matrix, receiving eigenvalues and eigenvectors.

The study of armchair nanoribbons

Based on tight-binding approximation, we present an analytical solution for energy and wave function of armchair nanoribbons. If we impose the border conditions on hard nanoribbon walls, we find that the wave function is discrete in the limited direction. This discrete wave vector is an indicator of different sub-ribbons. The structure of armchair nanoribbons has two atoms and two hard walls $(j=0,n+1)$ impose on the edges. The unit cell in this figure contains N atoms of A and B atoms [17]. In the tight-binding model, Bloch wave functions that relate to A and B atoms can be written as follows:

$$|k_x,p,A\rangle=\frac{1}{N_A}\sum_{i=1}^{n}\sum_{x_{Ai}}\exp(ik_x.x_{Ai})\phi_A(i)|A_i\rangle$$
$$|k_x,p,B\rangle=\frac{1}{N_B}\sum_{i=1}^{n}\sum_{x_{Bi}}\exp(ik_x.x_{Bi})\phi_B(i)|B_i\rangle \quad (11)$$

where $\phi_A(i)$ and $\phi_B(i)$ are the functions that should determine through border condition. $|A_i\rangle$ and $|B_i\rangle$ are atomic orbital wave functions in the proximity of A and B atoms in two atomic bases. We use border conditions to obtain $\phi_A(i)$ and $\phi_B(i)$ to introduce two $(j=0,n+1)$ borders:

$$\phi_A(j=0)=\phi_B(j=0)=0$$
$$\phi_A(j=n+1)=\phi_B(j=n+1)=0 \quad (12)$$

By selecting $\phi_A(i)=\phi_B(i)=\sin(\frac{\sqrt{3}q_y a}{2}i)$ and substituting it in equation 12, we have:

$$\phi_A(i)=\phi_B(i)=\sin(\frac{\sqrt{3}}{2}q_y ai)\Rightarrow\ \phi_A(n+1)=\phi_B(n+1)=\sin(\frac{\sqrt{3}}{2}q_y a(n+1))$$
$$\frac{\sqrt{3}}{2}q_y a(n+1)=p\pi\Rightarrow q_y=\frac{2}{a\sqrt{3}}\frac{p\pi}{n+1}\qquad \text{p=1,2,...}$$
$$\Rightarrow\phi_A(i)=\phi_B(i)=\sin(\frac{p\pi}{n+1}i) \quad (13)$$

a is the bond length between A and B atoms in the mesh. We use normalization condition to obtain N_A and N_B normalized coefficients:

$$\langle k_x,p,A|k_x,p,A\rangle=\langle k_x,p,B|k_x,p,B\rangle=1\Rightarrow N_A=N_B=\sqrt{\frac{N_x(n+1)}{2}} \quad (14)$$

N_x is the number of unit cells along the x. The equation (11) becomes as follows:

$$|k_x,p,A\rangle\sqrt{\frac{2}{N_x(n+1)}}\sum_{x_{Ai}}\sum_{i=1}^{n}e^{ik_x x_{A_i}}\sin(\frac{\sqrt{3}q_y a}{2}i)|A_i\rangle$$
$$|k_x,p,B\rangle=\sqrt{\frac{2}{N_x(n+1)}}\sum_{x_{Bi}}\sum_{i=1}^{n}e^{ik_x x_{B_i}}\sin(\frac{\sqrt{3}q_y a}{2}i)|B_i\rangle \quad (15)$$

The wave function of the ribbon can be obtained from the linear combination of $|k_x,p,A)\rangle$ and $|k_x,p,B)\rangle$:

$$|\psi\rangle=C_A|k_x,p,A\rangle+C_B|k_x,p,B\rangle\Rightarrow$$
$$C_A\left(\sqrt{\frac{2}{N_x(n+1)}}\sum_{xA_i}\sum_{i=1}^{n}e^{ik_x xA_i}\sin\left(\frac{\sqrt{3}q_y a}{2}i\right)|A_i\rangle\right)+$$
$$C_B\left(\sqrt{\frac{2}{N_x(n+1)}}\sum_{xB_i}\sum_{i=1}^{n}e^{ik_x xB_i}\sin\left(\frac{\sqrt{3}q_y a}{2}i\right)|B_i\rangle\right) \quad (16)$$

In armchair nanoribbons, by assuming anisotropy, we consider electron jump integration $t_{i,j}=t$. By substituting equation 16 and system Hamiltonian in the Schrodinger equation, we obtain the following formula:

$$\begin{bmatrix}\langle k_x,p,A|H|k_x,p,A\rangle & \langle k_x,p,A|H|k_x,p,B\rangle\\ \langle k_x,p,B|H|k_x,p,A\rangle & \langle k_x,p,B|H|k_x,p,B\rangle\end{bmatrix}\begin{bmatrix}C_A\\C_B\end{bmatrix}=E\begin{bmatrix}C_A\\C_B\end{bmatrix}$$
$$\Rightarrow\begin{bmatrix}\Delta & F\\ F^* & -\Delta\end{bmatrix}\begin{bmatrix}C_A\\C_B\end{bmatrix}=E\begin{bmatrix}C_A\\C_B\end{bmatrix}\rightarrow\begin{bmatrix}\Delta-E & F\\ F^* & -\Delta-E\end{bmatrix}\begin{bmatrix}C_A\\C_B\end{bmatrix}=0 \quad (17)$$

The final form of armchair nanoribbon is as follows:

$$E_+(k_x,p)=+\sqrt{\Delta^2+t^2(1+4\cos^2(\frac{p\pi}{n+1})+4\cos(\frac{p\pi}{n+1})\cos(\frac{k_x}{2}a)}$$
$$E_-(k_x,p)=-\sqrt{\Delta^2+t^2(1+4\cos^2(\frac{p\pi}{n+1})+4\cos(\frac{p\pi}{n+1})\cos(\frac{k_x}{2}a)} \quad (18)$$

The calculation of Hamiltonian functions

The following equation holds for armchair nanoribbon function:

$$\begin{bmatrix}\Delta & F\\ F^* & -\Delta\end{bmatrix}\begin{bmatrix}C_A\\C_B\end{bmatrix}=+\sqrt{\Delta^2+FF^*}\begin{bmatrix}C_A\\C_B\end{bmatrix}\rightarrow\begin{matrix}\Delta C_A+FC_B=+\sqrt{\Delta^2+FF^*}C_A\\ F^*C_A-\Delta C_B=+\sqrt{\Delta^2+FF^*}C_B\end{matrix} \quad (19)$$

Using equation (19), we have:

$$C_B=\frac{\left(\sqrt{\Delta^2+FF^*}-\Delta\right)}{F}C_A \quad (20)$$

As a result, the wave function is as follows:

$$|\psi\rangle=C_A|k_x,p,A\rangle+C_B|k_x,p,B\rangle=C_A\left\{|k_x,p,A\rangle+\frac{\left(\sqrt{\Delta^2+FF^*}-\Delta\right)}{F}|k_x,p,B\rangle\right\} \quad (20)$$

Therefore, wave functions will be obtained in index space after normalization:

$$|\psi_{(k_x,p)}\rangle_{\pm}=\frac{1}{\sqrt{2+\frac{2}{FF^*}\left(\Delta^2-\Delta\sqrt{\Delta^2+FF^*}\right)}}\left\{|k_x,p,A\rangle\pm\left(\frac{\sqrt{\Delta^2+FF^*}-\Delta}{F}\right)|k_x,p,B\rangle\right\} \quad (21)$$

$\pm$ indicates conductivity and capacity bands [47].

The density of states of armchair nanoribbons

The density of energy state is the most important measurable quantity. The concept of D (E) density of states is used to express the number of electron energy states in the conductivity band. In other words, D (E)dE indicates the

number of energy states of the electron in which E to E+dE interval is on dE energy range. The equation of the density of states is as follows:

$$D(E)=\sum_{n,k}\delta(E-E_n(k_x,p)) \quad (22)$$

Where $\delta(E-E_{n,k})$ is an expression of the number of states that their energy is in E range If the density of states becomes zero in surface energy or chemical potential $D(E=\mu=\varepsilon_F)=0$, the system takes non-metallic property and if it is not zero $D(E=\mu=\varepsilon_F)\neq 0$, the system shows metal property or conductivity. It is worth noting that the density of states relates to band structure by the following equation:

$$D(E)=-\frac{1}{2\pi N}\mathrm{Im}\sum_{k_{x,p,n=\pm}}\frac{1}{E-E_n(k_x,p)+i0^+} \quad (23)$$

Heat capacity of armchair nanoribbons

Heat capacity is the amount of heat given to the system to increase the system temperature up to 1 degree. Heat capacity is shown by C. Heat capacity concept applies only in cases where heat exchange with the system only changes the system temperature. The heat capacity equation is as follows:

$$C_v=\frac{\partial U}{\partial T}=\int_{-\infty}^{\infty}dE\,E\,D(E)\frac{\partial f(E)}{\partial T} \quad (24)$$

By having the density of the state of a material, we can calculate its heat capacity [57].

Where U is the internal energy of the system with the following equation:

$$U=\int_{-\infty}^{\infty}D(E)Ef(E)dE \quad (25)$$

And $f(E)$ is the Dirac function.

Findings

Heat capacity of armchair nanoribbons

Heat capacity of armchair nanoribbons for n different width is drawn based on k_BT/t.

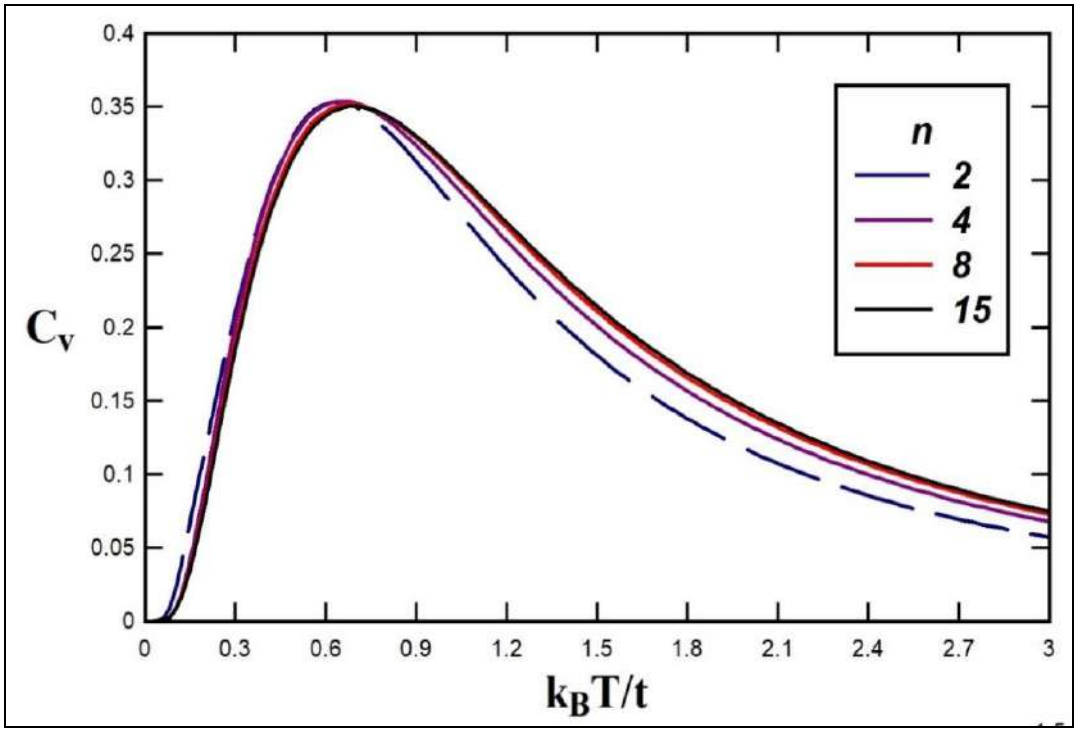

Diagram 1: Heat capacity of graphene armchair nanoribbons based on temperature for different n widths

As seen in diagram (1), by increasing the width of nanoribbon, the heat capacity increases in low temperature and decreases in high temperature. The increase of nanoribbon width finally increases the heat capacity in a fixed temperature above peak.

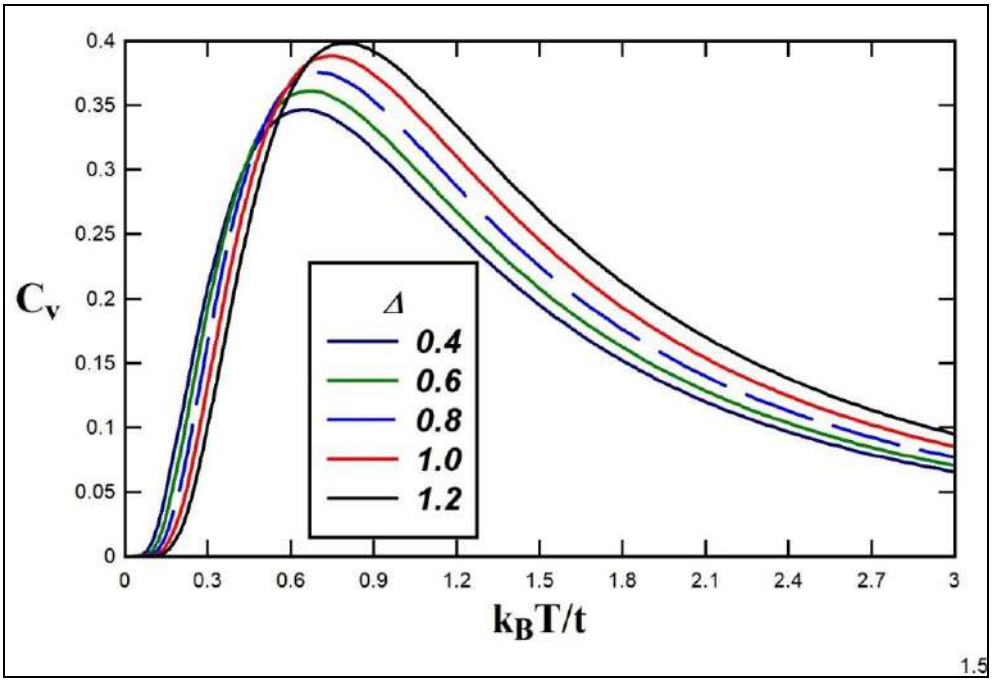

Diagram 2: heat capacity of graphene armchair nanoribbon based on temperature for width n=4 in different gaps

As seen, diagram (2) indicates a new property for heat capacity based on gap parameter i.e. heat capacity shows an increase higher than peak by increasing the gap. However, in temperatures lower than peak the heat capacity decreases by increasing the gap. This is consistent with Schottky law. According to this law, heat capacity in low temperatures corresponds with $e^{-\Delta/k_BT}$.

The effect of chemical potential on the thermal behavior of the heat capacity of nanoribbon with n=4 width is shown in figure (3) in the absence of a gap. This figure shows that a peak is seen foe each chemical potential value in the thermal behavior of heat capacity such that by increasing the chemical potential, the peak moves downward. The heat capacity decreases in a fixed temperature up to 0.9 by increasing chemical potential.

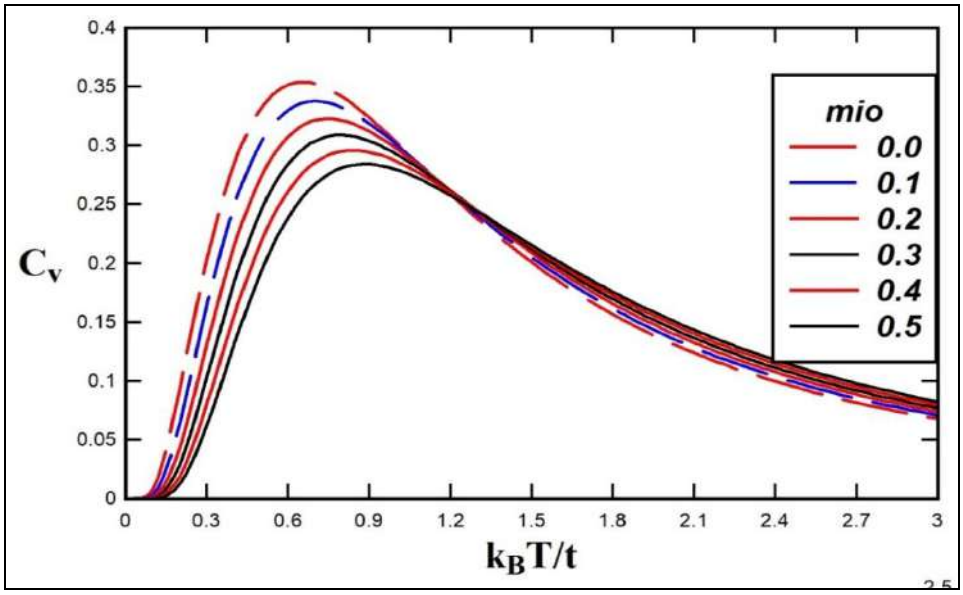

Diagram 3: dependence of heat capacity of graphene armchair nanoribbon to temperature for n=4 width with different chemical potentials

The density of armchair nanoribbons

Using the eigenvalues obtained for nanoribbons as well as density of states formula (DOS), the density of states of armchair nanoribbons can be drawn based on energy as diagram 4.

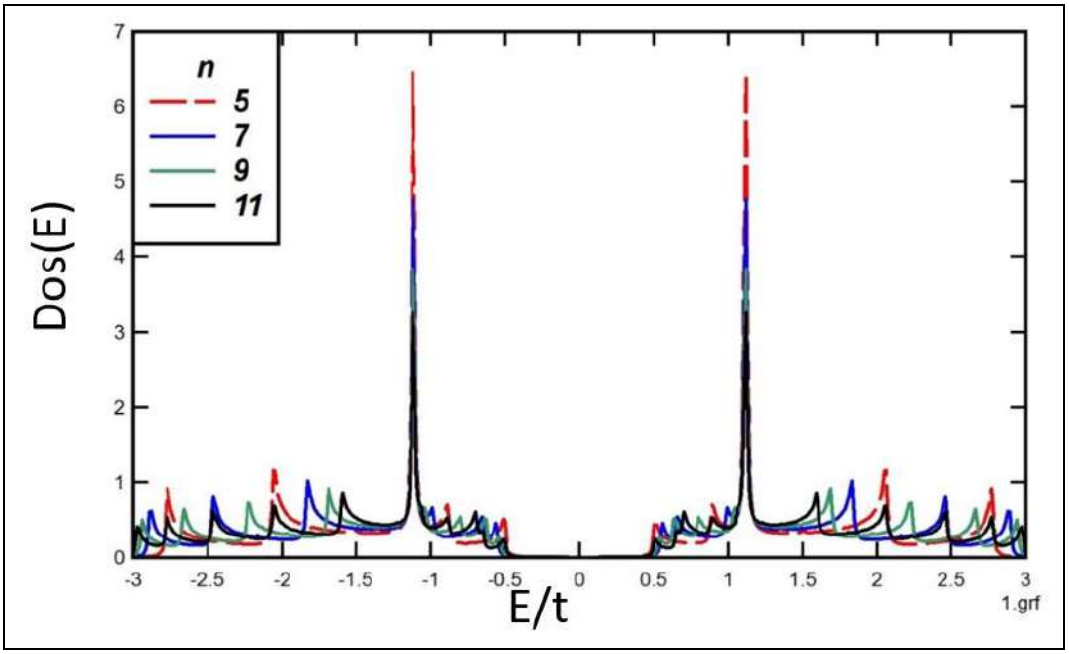

Fig 4: density of states (DOS) of armchair nanoribbons based on energy (E) for different n widths

Diagram 4 indicates that the density of states of armchair nanoribbons with different n widths has two high peaks. This indicates high energy states for electron. In an energy width near zero energy, the density of states becomes zero. These energy gaps indicates that these widths are insulated.

Conclusion

This research studied the effects of heat capacity gap on the insulation phase transition and developing a bandgap in the density of states and its effect on the thermal behavior of thermodynamic properties. The numerical results of Fortran programming analyzed by standard software. The effects of nanoribbon width on the density of states and thermal behavior of electrical conductivity studied. According to the obtained results about heat transfer, by increasing the width of nanoribbons, the heat capacity in low temperatures increases and higher temperatures decreases. Increasing the width of nanoribbons will increase the heat capacity at a fixed temperature at the peak. The heat capacity shows an increase in temperatures higher than peak by increasing the gap. Although in a temperature lower than peak, the heat capacity decreases by increasing the gap. This is consistent with Schottcky's law. On the other hand, the density of states of armchair nanoribbon with n different widths has two high peaks that indicates a high number of energy states for electron. In an energy width near zero energy, the density of states is zero. This energy gap indicates that these widths are insulated.

References

1. Park S, Ruoff RS. Chemical methods for the production of graphene, Nat. Nano 2009;4:217.
2. Berger C, Song Z, Li X, Wu X, Brown N, Naud C *et al.* A.de Heer, Electronic confinement and coherence in patterned epitaxial graphene, Science 2006;312:1191.
3. Neill AO, Khan U, Nirmalraj PN, Boland J, Coleman JN. Graphene dispersion and exfoliation in low boiling point solvents The journal of physical Chemistry 2011;115:5422.
4. Kabir E *et al*. Environmental impacts of nanomaterials. Journal of Environmentol Management 2018;225:261-271.
5. Klier N, Shallcross S, Sharma S, Pankratov O. Ruderman-Kittel-Kasuya Yosida interaction at finite temperature: Graphene and bilayer graphene, Phys. Rev. B 2015;92-205414.
6. Rafii-Tabar H. Computational modelling of thermo-mechanical and thansport properties of Carbon nanotubes, physics Reports 2004, 235-452.
7. Mahan GD. Many Particle Physics, 3nd ed. Academic Plenum Publishers 2000.
8. Zare M, Parhizgar F, Asgari R, Rkk Y. Interaction in the topological phase of zigzag silicone nanoribbon, ar Xiv, 2015, 1507-00899.
9. Novoselov KS, Geim AK, Morozov SV *et al.* Two-dimensional gas of massless Dirac fermions in Graphene, Nature 2005, 197–200.
10. Cano-Marquez AG, Rodriguez-Macias FJ, Campos-Delgado J, Espinosa Gonzalez CG, Tristan-Lopez F, YI D *et al.* Vega-Cantu, Nano Lett1 2009, 527-1533.
11. Peighambarian N, Etfan Coach, Andre Mizirovhich. An introduction to semiconductor optics. Hamidreza Jari Moghadam & Habib Tajali. Astan Qods Razavi 2001.
12. Wiley JS. Inc. Density Functional Theory 2009, 22-25.
13. DB Shinde, J Debgupta, A Kushwaha, M Aslam, VK Pillai, J Am. Chem. Soc 2011;133:4168–4171.
14. Imamura H, Bruno P, Utsumi Y. Twisted exchange interaction between localized spins embedded in a one- or two-dimensional electron gas with Rashba spin- orbit coupling, Physical Review B 2004;69:121303.
15. Jiao L, Zhang L, Ding L, Liu J, Dai H. Nano Res 2010;3:387–39.
16. M Saiz-Bretin, AV Malyshev, F Dominguez-Adame, D Quigley, RA Ro¨mer, D Quigley. Lattice thermal conductivity of gtaphene nanostructures, Carbon 2017.
17. Rezania H, Abdi A. Dynamical and Static Spin Susceptibilities of Doped Gapped Graphene Nanoribbon Due to Local Electronic Interaction 2017.